# *Master and Slave Relationship Between Two Types of Self-Propagating Insulin Amyloid Fibrils*

Weronika Surmacz-Chwedoruk, Viktoria Babenko and Wojciech Dzwolak*

## Supporting Information

**1. Primary structures of BI and KR insulins**
**2. Additional FT-IR data**
**3. Additional kinetic data**

## 1. Primary structures of BI and KR insulins

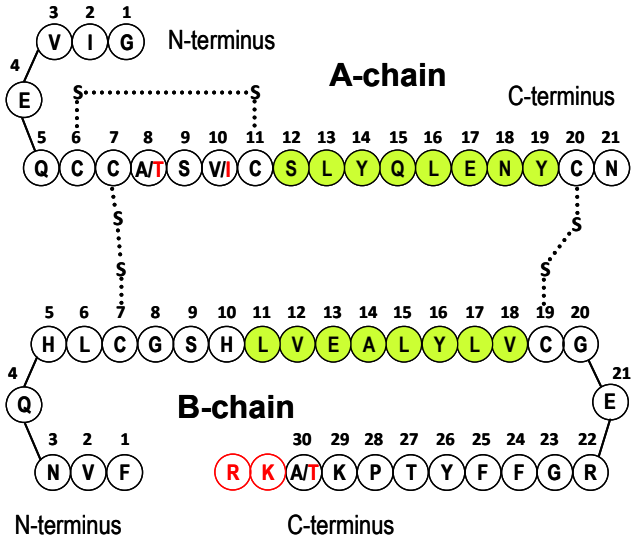


**Fig. S1** Amino acid sequences of BI and KR insulins. KR-specific substitutions are marked in red. Residues of two amyloidogenic regions are labelled with green filled circles (according to [S1-S2]).

## 2. Additional FT-IR data

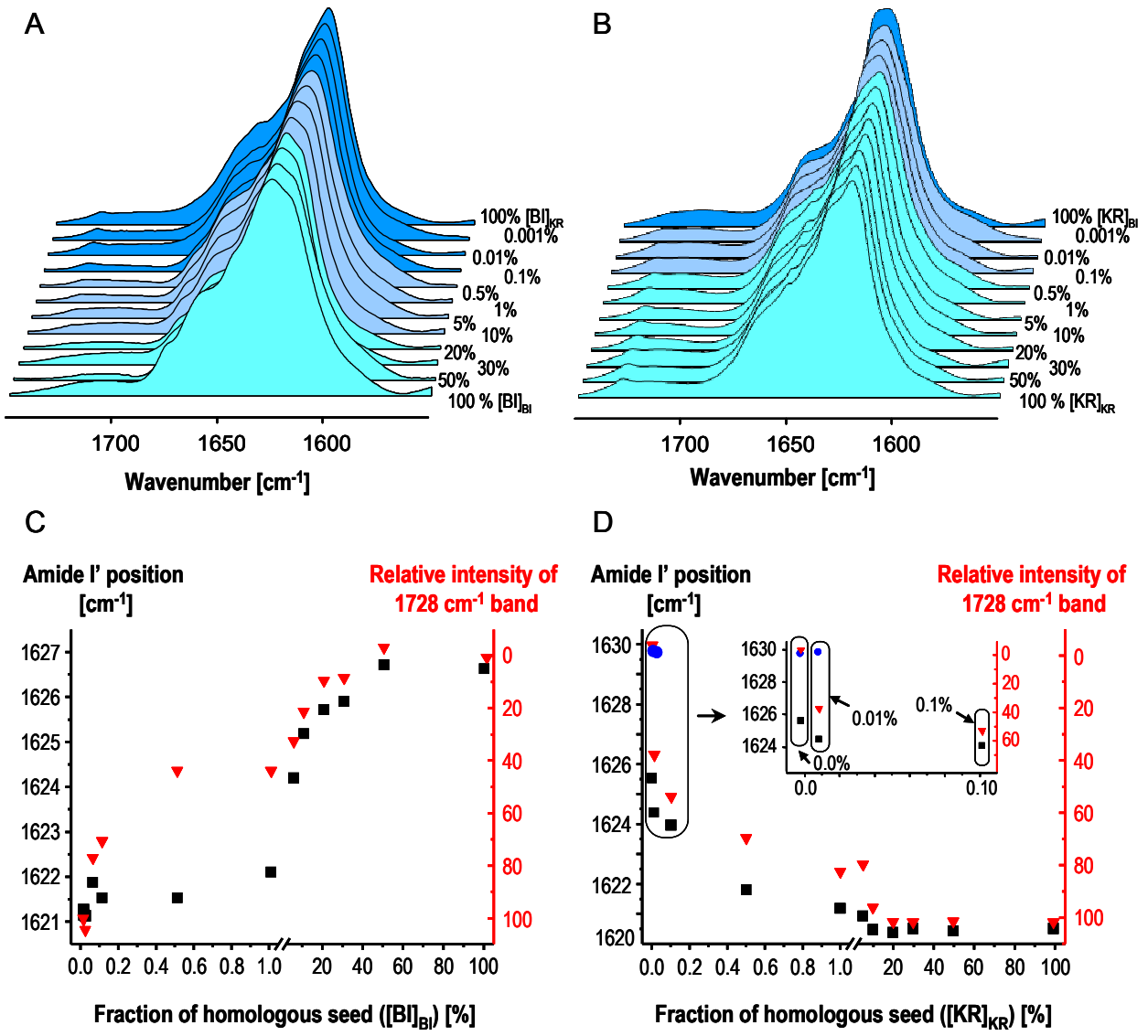


**Fig. S2 Figure is analogous to Figure 3 of the main paper but with all the spectral data acquired before sonication of daughter amyloid samples.** Infrared spectra of daughter [BI] (A) and [KR] (B) amyloid obtained through seeding native insulin with mixed fibrils at different [BI]/[KR] ratios. Percentages of homologous fibrils in seeds are indicated on the right side. The corresponding dependencies of amide I/I' band position (black squares) and intensity of 1728 $cm^{-1}$ peak (red triangles) on the fraction of homologous fibrils used for seeding BI and KR are plotted in panels (C) and (D), respectively. Region of extreme dilution of [KR] with [BI] upon seeding of KR (blue dots mark position of the lower intensity shoulder) is magnified in inset of panel D. Mass ratios of native insulin to total seed were fixed at 100:1.

# 3. Additional kinetic data

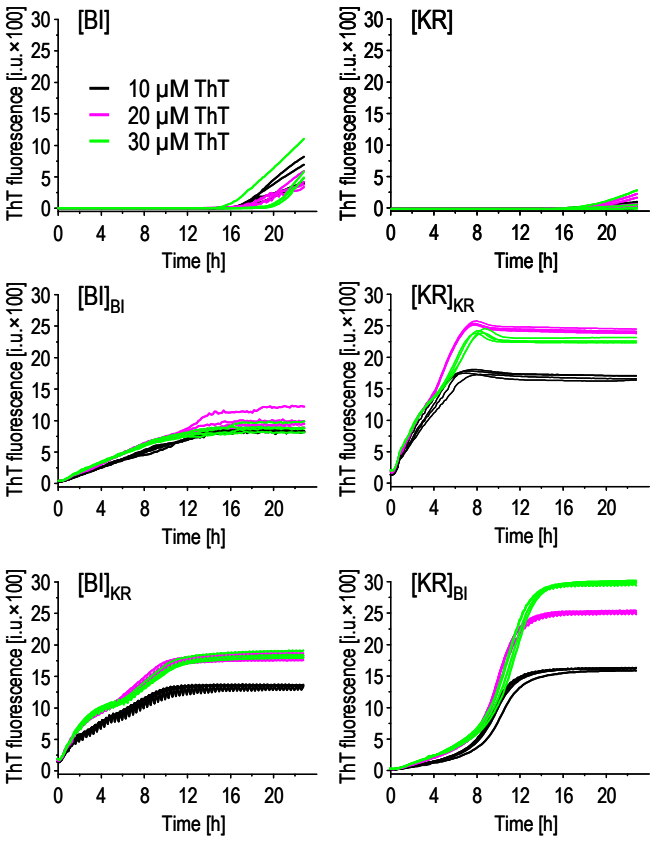


**Fig. S3 Spontaneous (top row), seeded (middle), and cross-seeded (bottom) fibrillation of BI and KR probed by Thioflavin T (ThT) fluorescence.** Kinetic measurements were carried out at 37 °C and gentle agitation at 300 rpm and in the presence of three different ThT concentrations. Multiple time traces correspond to several experiments being carried out simultaneously under identical conditions (in separate plate wells). Mass ratios of native insulin to total seed were fixed at 100:1.

Measurements were carried out at three different ThT concentrations in order to avoid possible misinterpretation of a final fluorescence plateau due to fluorophore depletion as false end of fibril elongation phase. The temporal coincidence of fluorescence saturation for samples containing 10, 20, and 30 μM ThT indicates that such artifacts were avoided and that the plateaus correspond to the completion of insulin aggregation. Long lag phases preceded onset of fibrillation in the absence of seeds. The gentle agitation applied continuously throughout fluorescence measurements accounts for the lag times of roughly 15-18h being still remarkably shorter than those inferred from the time-lapse FT-IR experiments (see Figure 4 of the main paper) with samples incubated under quiescent conditions.

There are several interesting (but lying beyond scope of this study) aspects of the data shown in Figure S3. For example, there are pronounced differences between final ThT fluorescence intensities of the four different types of daughter fibrils. We also note puzzling non-monotonic dependence of fluorescence intensity plateaus on ThT concentration in the case of $[KR]_{KR}$. Such effects are likely to arise from variations in number and conformation of accessible ThT-binding moieties, strength of fluorophore-fibril interactions, and local quenching mechanisms all of which are dependent on both fibril structure (imprinted by the seed) and its chemical composition (and therefore different for fibrils built of BI and KR). In each seeding/cross-seeding experiment, the rate of insulin fibrillation was strongly enhanced. Addition of homologous fibrils resulted in disappearance of lag phase which was followed by roughly linear increase of ThT fluorescence emission corresponding to the elongation phase which ended after 12 h for $[BI]_{BI}$, and 7 h for $[KR]_{KR}$.

More intricate kinetics were observed upon cross-seeding. When BI was seeded with [KR] elongation visibly decelerated after the first 3 hours. On the other hand, a significant acceleration was observed after 6 hours of KR fibrillation in the presence of [BI]. In both cases fibrillation begins with the rate characteristic for the seed and changes towards the rate typical for the seeded insulin. Should the fibrillation rate be controlled (under the identical sample conditions, temperature, and agitation rates) by the conformation of elongating fibril, then "conformational switching" towards wild type fibrils (i.e. mother-like [BI] and [KR]) could explain these nonlinearities. Of course, such transition would necessarily compromise fidelity of the conformational imprinting effect. However, control FT-IR measurements of cross-seeded daughter fibrils collected from the plate reader afterwards revealed no evidence supporting this scenario (Figure S4).

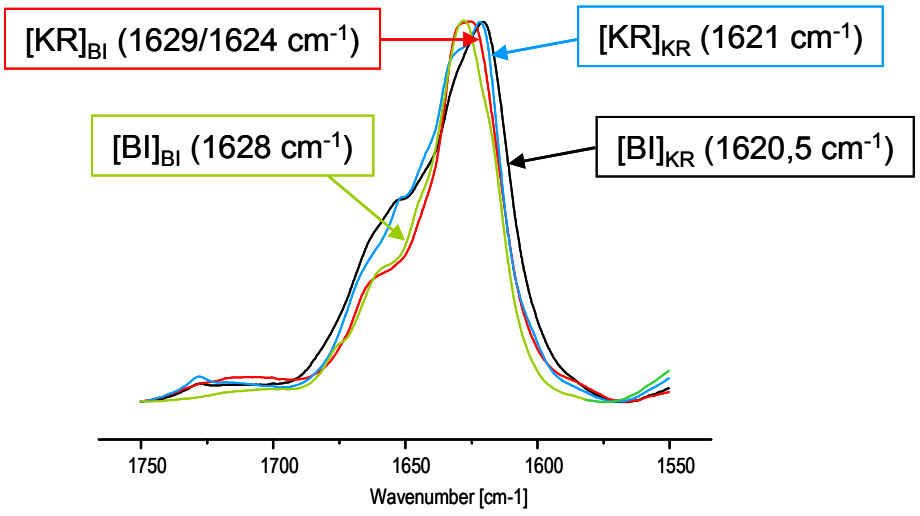


**Fig. S4 FT-IR spectra of daughter fibrils formed through seeding experiments shown in Fig. S3.** Samples for FT-IR spectroscopy were collected from plate wells afterwards.

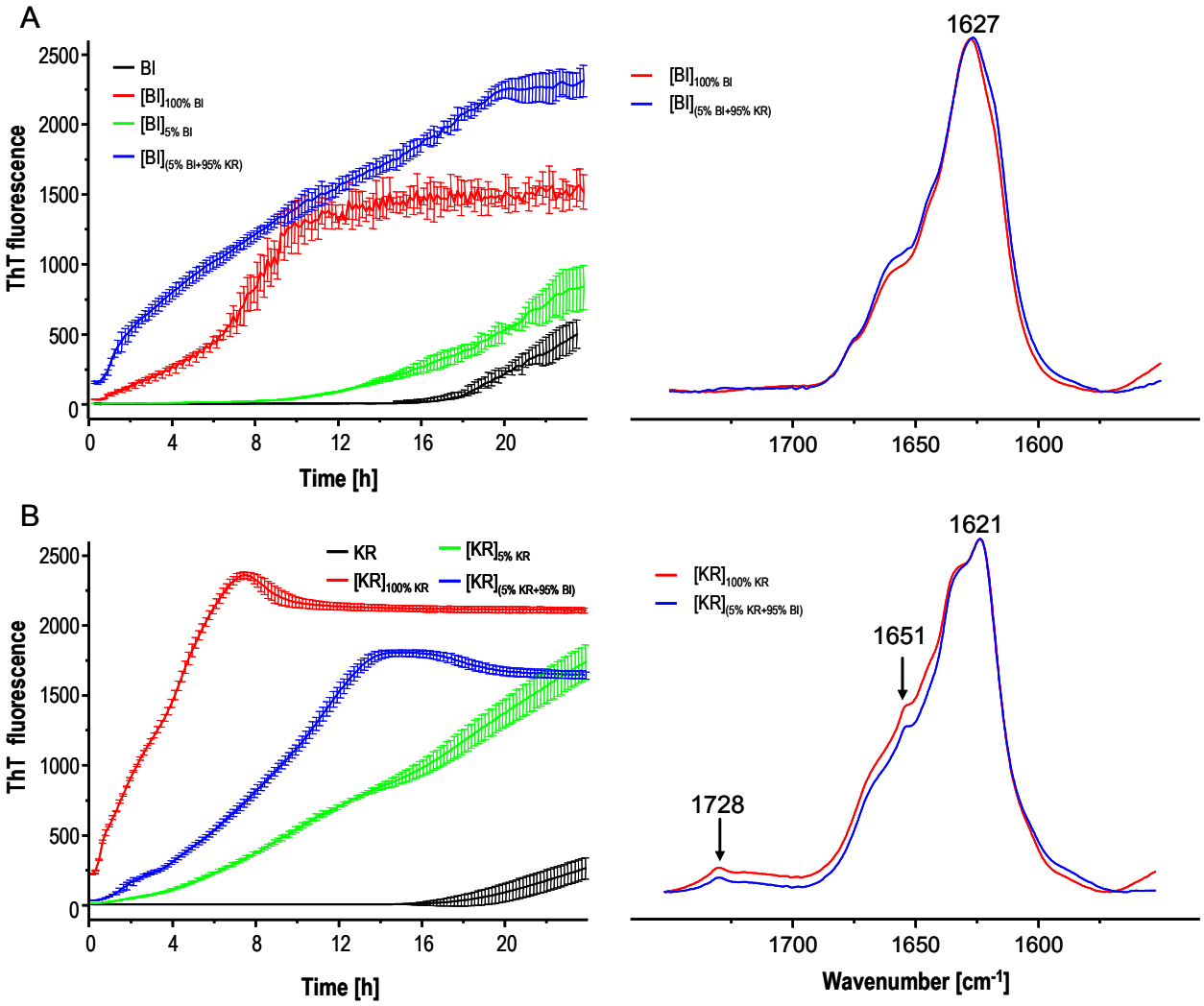


**Fig. S5 ThT fluorescence-monitored kinetics of seeding with mixed [BI] + [KR] templates.** Left panel: Kinetic traces of different seeding scenarios of BI (A) and KR (B) probed by ThT fluorescence at 37 $^{o}$C/300 rpm (averages of six parallel experiments). ThT emission intensities of samples seeded with homologous templates at 100:1 (native:amyloid) mass ratio are marked in red, whereas those corresponding to samples seeded with ([BI]+[KR]) mixtures where 95 % of the homologous seed are replaced with heterologous fibrils are in blue. Kinetics of fibrillation triggered by likewise diluted homologous seeds but in the absence of heterologous templates are plotted in green (effective seeding ratio 1:2000). Traces corresponding to fibrillation in the absence of seeds are in black. Right panel: Infrared spectra of daughter [BI] (top) and [KR] (bottom) fibrils seeded with homologous and mixed (5% homologous + 95 % heterologous) seeds collected right after completion of the 24-hour-long kinetic experiments reported on the left panel (samples for FT-IR measurements were collected from microplate wells and briefly sonicated prior to placing them in $CaF_2$ cell and acquisition of the spectral data).

## Materials and Methods

*Kinetic measurements of ThT fluorescence*

Kinetics of seeded fibrillation was probed using ThT-fluorescence assay with Fluoroskan Ascent FL fluorometer equipped with a pair of $\lambda_{ex.}$ 440 nm / $\lambda_{em.}$ 485 nm optical filters and 96-well black microplates. Samples were 1 wt. % insulin solutions in 0.1 M NaCl in $D_2O$, pD 1.9 containing in addition 20 μM ThT (or as specified in Fig. S3). Directly before measurements the samples were seeded typically at 100:1 mass ratio (or as specified in Fig. S5) with sonicated templates at desired ratios which were carried out at 37 $^{o}$C and gentle agitation of 300 rpm. In order to assess reproducibility of aggregation kinetics, 6 microplate wells were filled with identical 170 μl sample portions for parallel measurements.

### References

[**S1**] Ivanova, M. I., Thompson, M. J. & Eisenberg, D. "A systematic screen of β2-microglobulin and insulin for amyloid-like segments" ***Proc. Natl Acad. Sci. USA*** 103 (2006) 4079-4082.
[**S2**] Ivanova, M. I., Sievers, S. A., Sawaya, M. R., Wall, J. S. & Eisenberg, D. "Molecular basis for insulin fibril assembly" ***Proc. Natl Acad. Sci. USA*** 106 (2009) 18990-18995.